Applied Surface Science 256 (2010) 6923–6927

Contents lists available at ScienceDirect

Applied Surface Science

journal homepage: www.elsevier.com/locate/apsusc

Effect of calendering on paper surface properties

P. Vernhes [a,c,*], M. Dubé [b], J.-F. Bloch [c]

[a] Art Conservation Research Center, Carnegie Mellon University, 700 Technology Drive, Pittsburgh, PA 15219, United States
[b] Centre Intégré en Pâtes et Papiers (CIPP), Université du Québec à Trois-Rivières, 3351 boul. Des Forges, Trois-Rivières, Québec, G9A 6L2 Canada
[c] Laboratoire de Génie des Procédés Papetiers (LGP2), CNRS/Institut Polytechnique de Grenoble (Grenoble INP), 461, rue de la papeterie, BP 65, 38402 Saint-Martin-d'Hères cedex 9, France

ARTICLE INFO

Article history:
Received 12 February 2010
Received in revised form 28 April 2010
Accepted 1 May 2010
Available online 7 May 2010

Keywords:
Calendering
Different scales
Natural Fibers
Paper
Topography

ABSTRACT

Calendering of paper is an industrial finishing process designed to smoothen its surface so as to improve gloss as well as printability. In this article, we describe how calendering affects paper roughness on both microscopic and macroscopic length scales. We also discuss how these modifications relate to the morphology of the fibers composing the paper sheets. The characterization of the surface is carried out using an optical profilometer and two different species of fibers, as well as their mixture, are used. We first show that calendering induces modifications of the surface on all length scales measured and that these modifications are related by straightforward transformations. We also show that these results hold for papers formed from a mixture of fibers.

1. Introduction

The surface properties of papers and boards play an important role in converting operations such as sizing or coating [1] as well as having a determinant influence on the gloss appearance of the surface [2–5] and the properties of the final printed product [6]. Root mean square roughness, a typical descriptor of surface height variations, is traditionally measured and used as an indicator of paper quality [7]. It is however well-known that roughness is only an average measure of surface variations and does not specify on which length scale these variations occur [8–10] and therefore must be expressed as a function of both the evaluation length [11] and on the discretization step [12,13].

Fiber deposition models [14,15] were developed. However, these models based on fiber deposition do not reproduce the surface roughness properties of real paper sheet [15]. We focus here on industrial material measurement. This is an important point for paper since it is known that its surface exhibits multi-scale behavior and hence cannot be described by a single parameter [9]. Like other materials, this has immediate practical applications for gloss, which depends crucially on the surface correlations [3,4,16]. The multi-scale nature of paper surface also becomes important in sizing or printing. These operations involve paper surface compression, which cannot be adequately described by usual theories based on a distribution of Gaussian asperities [17].

The origin of the multi-scale behavior of paper surface is still largely unknown and is of interest. This question can be explored through numerical simulations using fiber depositions algorithms. Such simulations can reproduce laboratory-made paper sheets. However, commercial paper sheets undergo calendering, an operation which consists in compressing the paper past the elastic threshold between two hard or soft rolls [18]. It is also customary that one or both rolls are heated. Calendering reduces the roughness of paper and generally increases the gloss properties of the surface [19].

A detailed comprehension of the effects of calendering on the scale-dependent roughness of paper is still lacking. In the paper, we explore this question by following the changes induced by calendering on the paper surface of laboratory paper sheets of controlled composition. The nature of the raw material used in the preparation of the sheet is also investigated, as the topographical properties are related to the morphological properties of the fibers. The plan of this paper is as follows. Section 2 details the fiber content of the laboratory hand-sheets as well as the calendering operations performed. The surface descriptors used are also described in this section. Section 3 details the results and conclusions are presented in Section 4.

* Corresponding author at: Laboratoire de Génie des Procédés Papetiers (LGP2), CNRS/Institut Polytechnique de Grenoble (Grenoble INP), 461, rue de la papeterie, BP 65, 38402 Saint-Martin-d'Hères cedex 9, France.
E-mail address: p.vernhes@yahoo.fr (P. Vernhes).

0169-4332/$ – see front matter © 2010 Elsevier B.V. All rights reserved.
doi:10.1016/j.apsusc.2010.05.004

Table 1
Main morphological characteristics of fibers.

	Alpha fibers	Scots Pine fibers
Average length (um)	533	1364
Average width (um)	18.8	31.6
Coarseness (mg/m)	0.20	0.071

2. Material and methods

2.1. Fiber characterization and paper preparation

One of the goals of the study is to explore the origins of the length scales encountered through a detailed analysis of the surface properties. We thus concentrated on two types of fibers with different characteristics as may be seen in Fig. 1: Alpha fibers, very short fibers and a sharper fiber distribution, and typical softwood furnishes composed of Scots Pine fibers. The properties of these fibers were analyzed with a standard fiber analyzer (Morphi®). The average fiber length and width as well as the coarseness of these two types of fibers are presented in Table 1, with the detailed length and width distribution shown in Fig. 2.

Fig. 2 and Table 1 show that the Scots Pine fibers are roughly two times thicker than Alpha fibers, while their length is roughly three times larger. Standard isotropic hand-sheets were made using these fibers. A set of hand-sheets consisting in a mixture 50/50 were also made.

2.2. Calendering conditions

The hand-sheets were calendared using the two metal rolls of a laboratory calendering machine using two different line pressures, P_{max} = 100 kN/m and $P_{max}/2$. In addition, the hand-sheets were also calendared at a fixed temperature at T = 100 °C and under a load $P_{max}/2$.

2.3. Surface measurements

Surface measurements were performed with an Infinite Focus Measurement Machine (IFM) which is an optical profilometer allowing measurement of the surface position at high depth of focus similar to the scanning electron microscopy (SEM) [9]. The surface is obtained as a two-dimensional matrix of points $Z(x,y)$, with a size of 1024 pixel × 1280 pixel. All measurements were performed with a resolution of 0.8 μm.

2.4. Surface descriptors

(i) The first descriptor of the surface is the function $S_q(l)$, the standard deviation of the surface for a square subset of area l^2 of the total surface area.

$$S_q(l) = \sqrt{\frac{1}{l^2}\sum_{x,y \in l}(Z(x,y) - \bar{Z})^2}, \tag{1}$$

where $\bar{Z}$ is the average of the surface. If the surface is isotropic, as it is the case for paper hand-sheets, the local width can be described through the single length l. In several cases, it is observed that the local width scales with distance as a power law, with an exponent χ often called the roughness exponent. This power law behavior holds until a certain crossover length l_X after which the local width saturates to a constant value that corresponds to S_q, the standard deviation of an interface with infinite extent [8].

$$S_q(l \ll l_X) \approx l^{\chi} \tag{2}$$

$$S_q(l \gg l_X) \approx S_q \tag{3}$$

Both the roughness exponent χ and the crossover length depend on the type of surface considered, on the type of treatment that the surface has received and on the way the surface was produced.

(ii) Another quantity of interest for several applications is the normalized correlation function, defined as follows:

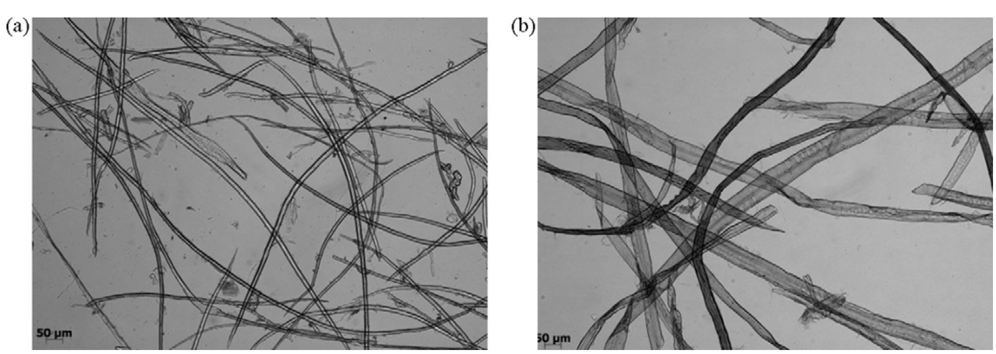

Fig. 1. Microscopic images of fibers: (a) Alpha and (b) Pine.

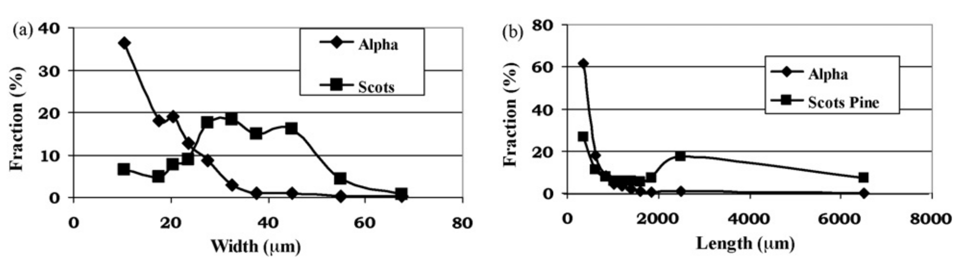

Fig. 2. Distribution of (a) fiber width and (b) fiber length.

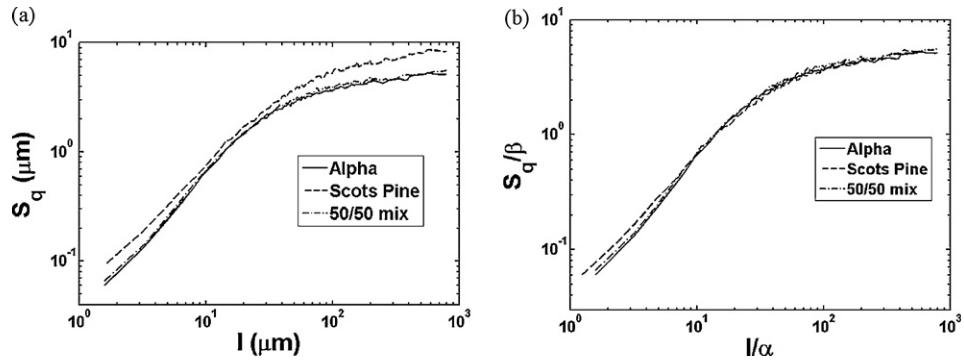

Fig. 3. (a) S_q as a function of system size for un-calendared hand-sheets composed of Alpha fibers, Scots Pine fibers and a 50/50 mix of both species. (b) Dimensionless S_q as a function of system size for un-calendared hand-sheets composed of Alpha fibers, Scots Pine fibers and a 50/50 mix of both species.

$$C_l(x,y) = \frac{\langle Z(x'+x, y'+y)Z(x',y')\rangle_l}{\langle Z(x',y')Z(x',y')\rangle_l} \quad (4)$$

Again, it is computed for a subset of area l^2 of the total area of the surface. The correlation function determines the extent of the correlations between two points on the surface separated by a distance (x,y). For an isotropic surface, it depends only on the radial distance $r^2 = x^2 + y^2$. As for the local width, a scaling form is usually observed.

$$1 - C_l(r \ll l_X) \propto \left(\frac{r}{l}\right)^{2\chi} \quad (5)$$

with $C_l(r \gg l_X) = 0$. From the correlation function, it is customary to extract the correlation length L_c, defined as the length at which the normalized correlation function reaches the value of $(1/e)$. This quantity is often used to relate several surface properties (e.g., gloss) to the surface characteristics. However, its use is justified only for surfaces which present an exponential decay of the surface. For a self-affine surface, it is clear that the correlation length is not a definite value, but rather scales with system size as follows:

$$L_c(l \ll l_X) \approx [\beta(1 - e^{-1})]^{1/2\chi} l \quad (6)$$

$$L_c(l \gg l_X) \approx [\beta(1 - e^{-1})]^{1/2\chi} l_X \quad (7)$$

The algorithms developed for the calculation of $S_q(l)$ and d $L_c(l)$ are straightforward and have been described previously [8,9].

3. Results

3.1. Surface properties of un-calendared hand-sheets

Fig. 3 shows $S_q(l)$ for un-calendered hand-sheets composed only of Alpha or Scots Pine fibers as well as a 50/50 mix of the two species. For all species, $S_q(l)$ initially increases (with a slope roughly equal to one) until it saturates to a constant value. Hand-sheets composed of Scots Pine fibers have a larger roughness than hand-sheets composed uniquely of Alpha fibers. It is however surprising to observe that the surface properties of hand-sheets composed of a mix of fibers are extremely close to those of hand-sheets composed only of Alpha fibers. It is not in the scope of this paper to explore this aspect. We rather focus on the effects of calendering on the surface properties. Nevertheless, it is possible that the similarity in the surface properties may be due to a lower settling velocity of Alpha fibers compared to Scots Pine fibers during the hand-sheet formation.

It is interesting to see that $S_q(l)$ for hand-sheets composed of Scots Pine fibers can be collapsed onto the values obtained for the ones composed of Alpha fibers through the following scaling transformation: $S_q(l) \to \beta^{-1} S_q(l/\alpha)$, as shown in the Fig. 3b. The value $\beta = 1.6$ corresponds to the ratio in the RMS roughness of the two hand-sheet while $\alpha = 4/3$ is closer to the ratio of the fiber width (see Table 1). The crossover length for hand-sheets of Alpha fibers can be roughly estimated as $l_X \approx 100$ μm and $l_X \approx 120$ μm for hand-sheets composed of Scots Pine fibers.

The characteristics of the un-calendered surfaces are further explored in Fig. 4. We first show the value of the logarithmic derivatives of the functions $S_q(l)$ for the various species:

$$\chi = \frac{d}{d(\log(l))} \log(S_q(l)). \quad (8)$$

For a self-affine fractal, the value of the derivatives yields the roughness exponent χ [8]. The value of the slope is initially close to one and drops to a near-zero value after a length $l = 75$ μm. It is however clear that the surfaces cannot be considered as true self-affine fractal since a constant value of χ cannot be observed on any length interval. Fig. 4b shows how the correlation length varies as

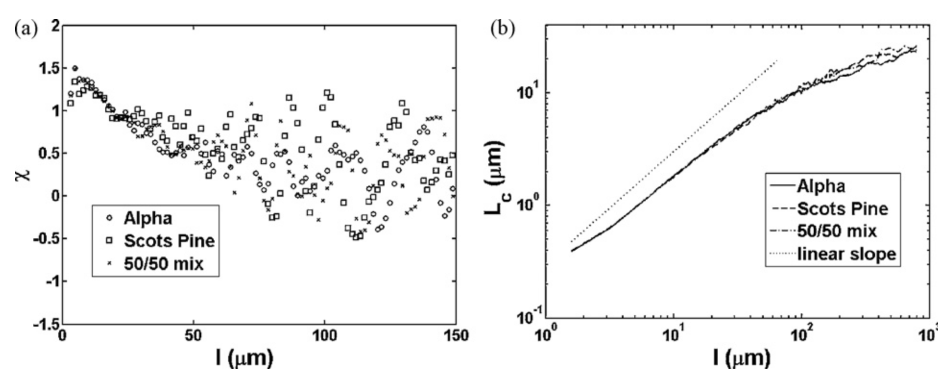

Fig. 4. (a) Logarithmic slope of S_q as a function of system size for un-calendared hand-sheets composed of Alpha fibers, Scots Pine fibers and a 50/50 mix of both species. (b) Correlation function as a function of system size for un-calendared hand-sheets composed of Alpha fibers, Scots Pine fibers and a 50/50 mix of both species.

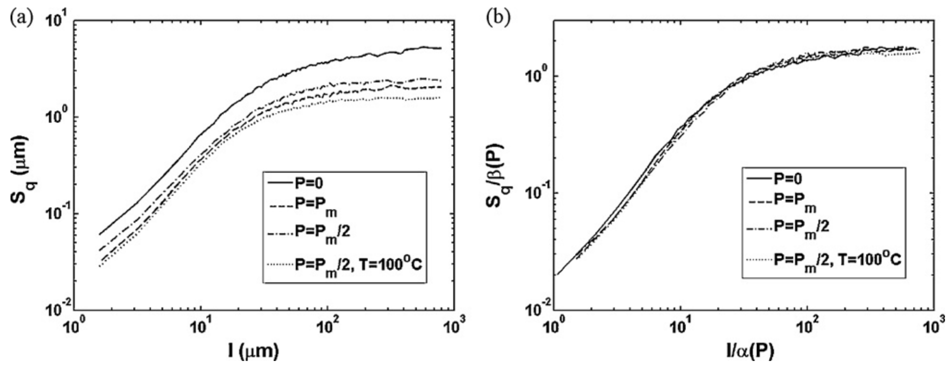

Fig. 5. (a) S_q as a function of system size for calendared hand-sheets composed of Alpha fibers and (b) normalized values of S_q.

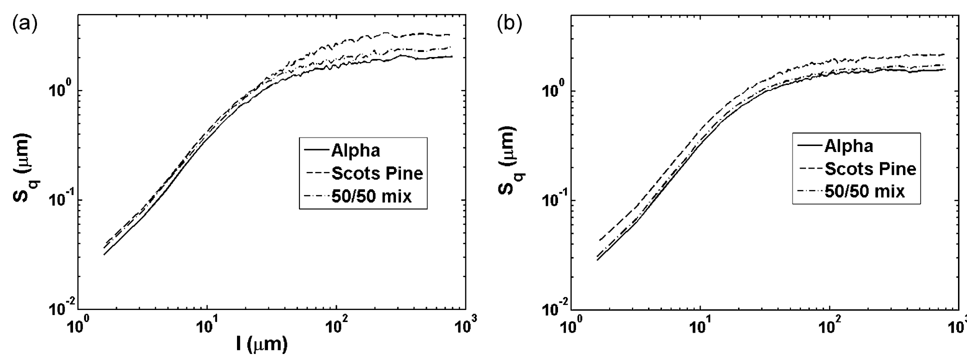

Fig. 6. S_q as a function of system size for calendared hand-sheets composed of various compositions: (a) $P = P_m$ and (b) $P = P_m/2$ and $T = 100\,^\circ$C.

a function of scale. The short scale behavior of $L_c(l)$ is independent of the hand-sheet composition, being roughly linear. The scaling described in Eq. (6) thus holds, even though the surfaces are not true self-affine surfaces. At larger scale, the different behavior of L_c simply reflects the different crossover length l_X as well as the slight increase in $S_q(l)$ that can still be observed for $l \gg l_X$.

3.2. Surface modification due to calendering

We now discuss how calendering modifies the surface properties of the hand-sheets. Fig. 5a shows how calendering affects the local roughness function $S_q(l)$ for hand-sheets composed of Alpha fibers.

Calendering reduces roughness on all scales. The crossover length is only very slightly affected by calendering, the most noticeable effects being the general decrease of roughness. This is not too surprising since it is already known that the mechanical Poisson ratio of paper is very small [20], that is to say that there is no planar deformation due to a transverse compression. It is however interesting to notice that the shape of the curve is similar for all levels of calendering, including the one dedicated to the modification of temperature. As for un-calendered hand-sheets, it is possible to perform a scaling transformation of all curves and collapse them on a single scaling function, as shown in Fig. 5b. The scaling factors, β and α, are close to 1, since all the curves are similar in the first place. This is nevertheless an unexpected and intriguing new result.

Table 2 shows how calendering affects large scale roughness for all hand-sheets considered in the study. It is clear that hand-sheets composed of Alpha fibers are always the smoothest and those composed of Scots Pine only are the roughest, independent of the calendering operation. The table also shows that the roughness with furnishes composed of both Alpha and Scots Pine fibers has a roughness closer in value to those of hand-sheets composed uniquely in Alpha fibers, and this for all types of calendering operations. This is confirmed in Fig. 6 which shows $S_q(l)$ for the three types of furnishes under two different calendering loads. The smoothest surfaces are produced by calendering with a temperature gradient, an operation which also reduces greatly

Table 2
Large scale roughness of the hand-sheets with the three furnishes under consideration. The value of $S_q(\infty)$ is obtained from averaging the values of $S_q(l)$ from $l = 530\ \mu$m to $l = 1000\ \mu$m, with the number in parentheses consisting on the standard deviation of the value.

	$S_q(\infty)$ (μm)		
	Alpha fibers	50/50 mix	Scots Pine fibers
$P = 0$	5.14 (0.07)	5.3 (0.2)	8.3 (0.2)
$P = P_m/2$	2.42 (0.04)	2.86 (0.04)	3.1 (0.1)
$P = P_m$	2.02 (0.03)	2.40 (0.07)	3.28 (0.04)
$P = P_m/2$, $T = 100\,^\circ$C	1.55 (0.02)	1.71 (0.03)	2.15 (0.02)

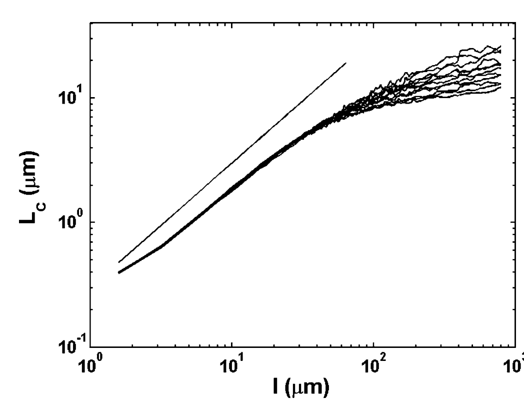

Fig. 7. Correlation length for Alpha fibers, considering different pressure and temperature conditions.

the differences introduced by the different furnishes. It is clear that there is very little difference between the curves of Fig. 6b, obtained from a calendering load $P_m/2$ and $T = 100\,^\circ\mathrm{C}$, and the curves of Fig. 6a, obtained under a single load $P = P_m$ without any heating. Although not shown, all curves can also be collapsed through appropriate scaling transformations.

3.3. Effects of calendering on the correlation length

Fig. 7 shows how the correlation length, defined for a system of size l, varies with calendering for all furnishes and calendering conditions. The behavior is extremely similar in all cases, minor differences arising only at large scales due to different overall roughness levels and crossover lengths.

4. Conclusion

We first showed that non-calendared hand-sheets possess a self-affine structure up to a definite crossover length scale. Our results show that calendering reduces surface variations on all length scales, with only a minor change on the crossover length. We further show that the surface properties of the calendared hand-sheet can be related to those without calendering by a simple scaling transformation. This transformation can be done for hand-sheets of various compositions and calendering conditions. Finally, we observed that the modifications induced by calendering are quite independent of the composition of the hand-sheets. The detailed properties of the fibers will influence the overall value of the roughness, but not the shape of length-dependent roughness $S_q(l)$.

Acknowledgements

The authors would like to thank B. Khelifi for the images of the fibers.

References

[1] E. Lehtinen (Ed.), Pigment Coating and Surface Sizing of Paper, Tappi Press, Atlanta, GA, 2000.
[2] G. Chinga, Detailed characterization of paper surface structure for gloss assessment, J. Pulp Pap. Sci. 30 (2004) 222–227.
[3] R. Alexandra-Katz, R.G. Barrera, Surface correlation effect on gloss, J. Polym. Sci. B: Polym. Phys. 36 (1998) 1321–1334.
[4] E. Caner, R. Farnood, N. Yan, Relationship between gloss and surface texture of coated papers, Tappi J. 7 (4) (2008) 19–26.
[5] P. Vernhes, A. Blayo, J. Bloch, B. Pineaux, Gloss optical elementary representative surface, Appl. Optics 47 (2008) 5429–5435.
[6] J.F. Bloch, S. Rolland du Roscoat, P. Verhnes, C. Mercier, B. Pineaux, A. Blayo, Influence of paper structure on printability: characterisation using X-ray synchrotron microtomography, Presented at NIP, Denver, USA, 2006.
[7] R. Xu, P.D. Fleming, A. Petrakarovicova, V. Bliznyuk, The effect of ink jet paper roughness on print gloss, J. Imaging Sci. Technol. 49 (6) (2005) 660–666.
[8] A.-L. Barabasi, H.E. Stanley, Fractal Concepts in Surface Growth, Cambridge University Press, 1995.
[9] P. Vernhes, A. Blayo, J. Bloch, B. Pineaux, Statistical analysis of paper surface microstructure: a multi-scale approach, Appl. Surf. Sci. 254 (2008) 7431–7437.
[10] M. Bigerelle, A. Gautier, A. Iost, Roughness characteristic length scales of micromachined surfaces: a multi-scale modelling, Sens. Actuators B 126 (2007) 126–137.
[11] R.M. Patrikar, Modeling and simulation of surface roughness, Appl. Surf. Sci. 228 (2004) 213–220.
[12] J.-J. Wu, Characterization of fractal surfaces, Wear 239 (2000) 36–47.
[13] S. Ganti, B. Bhusnan, Generalized fractal analysis and its applications to engineering surfaces, Wear 180 (1995) 17–34.
[14] J.D. Sherwood, H. Van Damme, Nonlinear compaction of an assembly of highly deformable platelike particles, Phys. Rev. E 50 (1994) 3834–3840.
[15] J. Vinnurva, M. Alava, T. Ala-Nissala, J. Krug, Kinetic roughening in fiber deposition, Phys. Rev. E 58 (1998) 1121–1131.
[16] U. Arino, G.G. Kleist, P.A. Barros, M. Johansson, Rigdahl, Surface texture characterization of injection-molded pigmented plastics, Polym. Eng. Sci. 44 (2004) 1615–1626.
[17] E. Lehtinen (Ed.), Papermaking Part 3, Finishing, Tappi Press, Atlanta, GA, 1999.
[18] Suontausta, O., 2002. Coating and calendering—means of improving surface of coated paper for printing, Ph.D. Thesis, Helsinki University of Technology, Espoo.
[19] P. Vernhes, A. Blayo, J. Bloch, B. Pineaux, Effect of calendering on paper surface micro-structure: a multi-scale analysis, J. Mater. Process. Technol. 209 (2009) 5204–5210.
[20] N. Stenberg, C. Fellers, Out-of-plane Poisson ratios or paper and paperboard, Nordic Pulp Pap. Res. J. 17 (4) (2002) 387–394.